PERGAMON

International Journal of Heat and Mass Transfer 44 (2001) 4185–4194

International Journal of HEAT and MASS TRANSFER

www.elsevier.com/locate/ijhmt

Constructal optimization of nonuniformly distributed tree-shaped flow structures for conduction

M. Almogbel, A. Bejan *

Department of Mechanical Engineering and Materials Science, School of Engineering, Duke University, Box 90300, Durham, NC 27708, USA

Received 25 October 2000; received in revised form 16 February 2001

Abstract

Constructal tree designs are hierarchical high-conductivity paths that minimize the global resistance between an entire volume and one point. In past work, the structure was optimized as a sequence of building blocks (volume sizes), which started with the smallest size (elemental volume) and continued toward larger and more complex assemblies (first construct, second construct, etc.). The resulting structure had a 'uniform' distribution of interstitial spaces, because the size of the elemental volume was fixed. In this paper we relax the elemental size constraint, and show that the added design freedom leads to significant improvements in global performance, i.e., to decreases in the global resistance to volume–point flow. Each tree structure, or the distribution of high-conductivity material through low-conductivity background, is optimized by simulating numerically and comparing large numbers of designs where the geometry changes smoothly from one design to the next. The results show that each optimized structure has not one but several elemental volume sizes, and that the volume elements situated far from the root of the tree are notably smaller. The resulting tree is nonuniform, i.e., denser near the periphery of its canopy. In sum, better global performance is achieved when the complexity and number of degrees of freedom of the structure are increased. In the same direction, the optimized nonuniform tree structure looks more and more natural.

Keywords: Constructal theory; Topology optimization; Dendrites; Trees; Networks; Self-organization; Self-optimization

1. Constructal design: uniform and nonuniform interstitial sizes

Tree-shaped flow paths are extremely common in engineered and natural flow systems. In every case the tree connects a volume to one point, where the point serves as source or sink. The visible channels that form the links (branches) of the tree are characterized by a flow resistance that is considerably lower than the resistance of the diffusive flow that sweeps the interstitial spaces between neighboring links. The channels are thicker near the root, and progressively thinner away from the root, near the smallest channel – the smallest volume element bathed by the smallest channel length scale of the tree network.

These geometric characteristics are universal, i.e., independent of what flows between the volume and the point (e.g., fluid, heat, electricity, goods, people). The vast array of natural and engineered flow systems that are shaped as trees stresses the universality of this geometric structure (e.g., lungs, vascularized tissues, river basins and deltas, lightning, dendritic crystals, urban traffic, electric power distribution lines, transportation routes) [1–10].

The formation of tree-shaped flow paths has been reasoned on the basis of a principle of global optimization of system performance subject to global constraints [1]. The system is the volume that is bathed at every point by the volume–point flow. The optimization of performance, i.e., the objective, is the minimization of the overall resistance encountered by the volume–point flow, or the maximization of the global thermodynamic

* Corresponding author. Tel.: +1-919-660-5309; fax: +1-919-660-8963.

E-mail address: dalford@duke.edu (A. Bejan).

0017-9310/01/$ - see front matter
PII: S0017-9310(01)00080-1

Nomenclature

A	size (area) of two-dimensional volume [m^2]
A_p	size (area) of volume occupied by high-conductivity inserts [m^2]
D	thickness of high-conductivity channel [m]
H	overall dimension perpendicular to the trunk [m]
k_p	high thermal conductivity [W/m K]
k_0	low thermal conductivity [W/m K]
$\tilde{k}$	ratio of thermal conductivities, k_p/k_0
L	overall dimension aligned with the trunk [m]
n_1	number of elemental volumes in the first construct
n_2	number of first constructs in the second construct
q'''	uniform rate of volumetric heat generation [W/m^3]
T	temperature [K]
(x, y)	Cartesian coordinates [m]
x_i	locations of the D_0-thin channels in the first construct [m], Eq. (7)
y_i	locations of the D_1-thin channels in the second construct [m]

Greek symbol

ϕ	volume fraction occupied by high-conductivity material, A_p/A

Subscripts

m	minimized
min	minimum
opt	optimum
peak	largest value
u	uniform
0	elemental volume
1	first construct
2	second construct
xm	minimized x times

Superscripts

˜	dimensionless notation, Eqs. (4) and (5)
ˆ	dimensionless notation, Eq. (7)

performance of the flow system. The global constraints are the fixed system volume and the fixed volume fraction occupied by all the channels. It was shown that the tree geometry can be deduced in every detail from the consistent application of the objective and constraints principle. The resulting tree structures constructed in this manner have been named *constructal designs*. The thought that the same objective and constraints principle stands behind the tree-shaped flow paths that occur in natural systems (animate and inanimate) has been named *constructal theory* [1,11].

In the first tree-shaped flows that were deduced from principle, the construction began with the geometric optimization of the smallest volume element of the system. The elemental volume contained only one channel, and its size was fixed. The optimized element became the smallest building block in a complex structure of progressively larger constructs (assemblies of elements, and assemblies of constructs). In the end, when this construction covered the entire system volume, the channels of all the elements and subsequent constructs formed a tree-shaped flow path. The volume was filled with elements of a single size, and the tree was the fingerprint of the construction, i.e., the manner in which the elements were assembled and connected optimally.

The single size of the elemental volumes assumed in the tree-flow systems deduced until now forced all the tree structures to have interstitial spaces of the same size. Said another way, the smallest links of the tree were distributed uniformly over the system volume. In the present paper we refer to a tree structure of this type as a *uniformly distributed tree*. The new proposal made in this paper is to relax the single-size assumption, and to consider elemental volumes the finite sizes of which may vary freely around a fixed characteristic volume scale. The flow structures that result are *nonuniformly distributed trees*.

Improvements in global performance can be expected when the uniform tree is refined and replaced by a nonuniform tree that satisfies the same global constraints. Improvements can be expected for two reasons. Theoretically, we showed that when a simplifying assumption such as the 90° angle between branches is relaxed, the angle can be optimized, and the global volume–point resistance is reduced [1]. Empirically, it is observed that all the tree-shaped flow paths that occur naturally have smaller elemental volumes (interstices) near the outer surface of the canopy, in regions situated the farthest from the root point. Indeed, in this paper we will show that the geometric optimization of a nonuniformly distributed system generates a structure that performs better than the uniform tree, and in which the optimized elemental volume sizes decrease as the distance from the root increases.

2. Numerical formulation

We studied the optimization of nonuniform tree structures in the context of steady two-dimensional heat conduction between a rectangular domain of fixed size

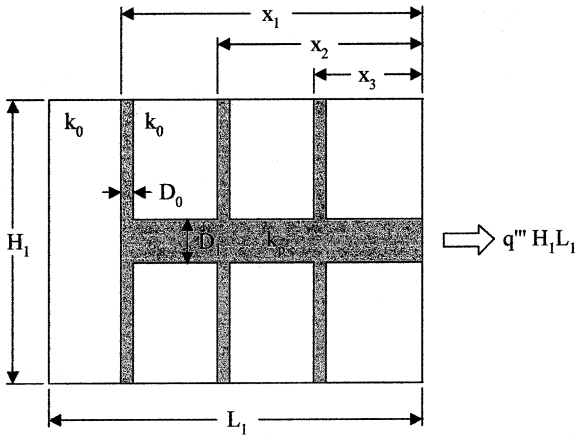

Fig. 1. First construct with nonuniformly distributed elemental volumes.

and one small patch on its boundary. To make the formulation of the problem more concrete, consider the rectangular space $H_1 \times L_1$ shown in Fig. 1, in which the shape parameter H_1/L_1 may vary. Heat is being generated uniformly at the rate q''' [W/m^3] over the entire domain. The heat current generated by the system ($q'''H_1L_1$) escapes through a boundary patch of width D_1, which in Fig. 1 serves as root for the darker tree-shaped area. The rest of the rectangular boundary is insulated.

The conductivity of the material that fills most of the system (the white spaces in Fig. 1) is relatively low, k_0. The thermal resistance encountered by the volume–point current is reduced significantly by inserting a small amount of high-conductivity (k_p) material. This material is shown in dark in Fig. 1: much of the geometric optimization work will be devoted to distributing this material optimally through the k_0 material. The resulting composite is a heterogeneous conductive medium characterized by two dimensionless parameters,

$$\tilde{k} = k_p/k_0 \gg 1, \tag{1}$$

$$\phi = A_p/A \ll 1, \tag{2}$$

where A_p and A are the areas that represent the two-dimensional volume of k_p material (the dark area in Fig. 1) and, respectively, the two-dimensional volume of the entire system (e.g., H_1L_1 in Fig. 1).

With reference to a Cartesian system where x is aligned with L_1 and y with H_1, the steady conduction phenomenon is governed by the energy equation

$$\frac{\partial^2 T}{\partial x^2} + \frac{\partial^2 T}{\partial y^2} + \frac{q'''}{k_0} = 0 \tag{3}$$

subject to the boundary conditions mentioned in the first paragraph of this section. The internal thermal resistance at the interface between the k_p and k_0 domains is neglected. Nondimensionalization is achieved by using $A^{1/2}$ as length scale, because the size A is fixed,

$$(\tilde{x}, \tilde{y}) = (x, y)/A^{1/2}, \tag{4}$$

$$\tilde{T} = \frac{T - T_{\min}}{q'''A/k_0}. \tag{5}$$

The difference $(T - T_{\min})$ is measured between the local temperature at a point inside the system, $T(x, y)$, and the temperature of the boundary patch that serves as heat sink ($T_{\min}$). The highest temperature that occurs at one or several points (hot spots) inside the system is T_{peak}, and the corresponding dimensionless temperature is

$$\tilde{T}_{\text{peak}} = \frac{T_{\text{peak}} - T_{\min}}{q'''A/k_0}. \tag{6}$$

Table 1
Comparison between the hot-spot temperature results of an elemental system calculated with the finite-elements and finite-volume codes ($\phi_0 = 0.1$, $H_0/L_0 = 1$)

$\tilde{k}$	FE	FV
8000	0.116699	0.115239
300	0.126351	0.124205
100	0.152859	0.150849
30	0.234971	0.233310
10	0.408175	0.407372

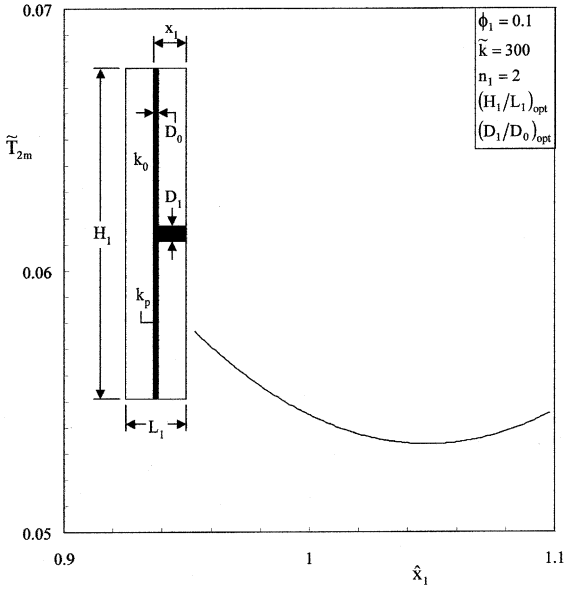

Fig. 2. The optimization of the position of the elemental channels in a first construct with only two elemental volumes ($n_1 = 2$, $\phi_1 = 0.1$, $\tilde{k} = 300$).

The numerical work began by assuming a certain configuration, and determining numerically the temperature distribution $T(x,y)$ in that configuration. For example, in Fig. 1 the assumed configuration is represented by the external aspect ratio H_1/L_1, the internal aspect ratio D_1/D_0, the number of elemental channels of thickness D_0 and their positions $(x_1, x_2, \ldots)$, and the number of channels of thickness D_1. The objective of the numerical simulation of heat conduction in the assumed configuration is the calculation of the peak temperature $(\tilde{T}_{\text{peak}})$, which is a property of the configuration.

The group $\tilde{T}_{\text{peak}}$ is proportional to the ratio $(T_{\text{peak}} - T_{\min})/q'''A$, which represents the *global* thermal resistance between the volume and the heat sink. This is a global measure of the performance of the volume–point flow because the current $q'''A$ is generated by the entire system, and the hot-spot temperature level T_{peak} is a feature of the system. Important in the thermal design of heat generating volumes (e.g., electronics packages) is the value of T_{peak} (the ceiling), not the particular location (x,y) of the point where T_{peak} may occur. The objective of the numerical work was to minimize the global resistance by making appropriate changes in the distribution of the high-conductivity (k_p) material through the low-conductivity (k_0) material. This procedure of topology optimization led to the nonuniform tree structures documented in the following sections.

The nondimensionalized conduction problem was solved by using a finite elements code (FE) [12], in conjunction with a mathematical solver. It was necessary to use this software because for this geometric optimization problem we needed a reliable and flexible FE solver capable of handling efficiently very large matrices. We needed to manage and automate the procedure of simulating a huge number of tree configurations, interpolating the results, and searching for the optimum values. During the optimization procedure the grids were nonuniform in both x and y, and their fineness was tested from one geometric configuration to the next. The grid was selected such that the dimensionless tempera-

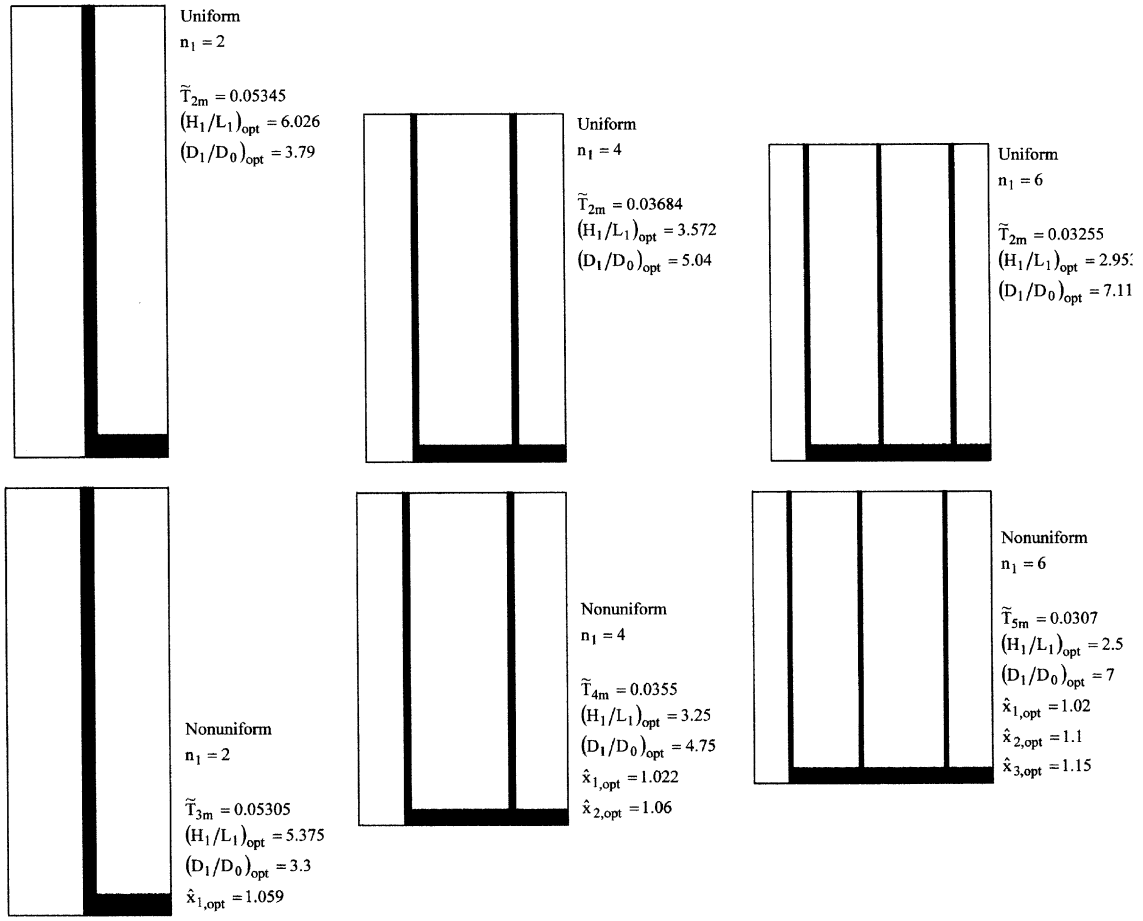

Fig. 3. Top: optimized first construct with uniformly distributed elemental volumes. Bottom: the corresponding optimized structures with nonuniformly distributed elemental volumes ($\phi_1 = 0.1$, $\tilde{k} = 300$).

ture results were insensitive to further grid doubling in both directions. Specifically, the grid was refined to as many as 20,000 nodes in some cases, to ensure that the further doubling of the number of nodes resulted in changes of less than 0.05% in the hot-spot temperature. The average number of nodes for all the simulations was 6000. Quadrilateral elements with biquadratic interpolation functions were used. The accuracy of the FE code was tested against a finite volume code (FV) based on the Cholesky back-substitution method: this test code was developed by the authors, and was used extensively [13]. Table 1 shows the close agreement between the hot-spot temperature ($\tilde{T}$ at $x = 0$ and $y = H_0/2$) calculated with the FE code and the corresponding values determined with the FV code.

3. First construct with nonuniform interstices

In this study the optimization of geometric form proceeded from simple first constructs toward more complex first and second constructs. We illustrate this sequence step by step, to show how the optimization program was built.

According to the constructal-design terminology, the first construct is an assembly of elemental volumes, where the elemental heat currents are collected by a single central channel (D_1 in Fig. 1). The simplest first construct has only two elemental volumes, i.e., only two channels of thickness D_0. This simplest configuration ($n_1 = 2$) is represented by three degrees of freedom: H_1/L_1, D_1/D_0 and the distance from the elemental channel to the root, $\tilde{x}_1 = x_1/A_1^{1/2}$, where $A_1 = H_1L_1$. Note that in the nondimensionalization of the problem, Eqs. (4)–(6), the role of system size (A) is played by A_1.

The dimensionless alternative to using $\tilde{x}_1$ as degree of freedom is to use the ratio $\hat{x}_1 = x_1/x_{1,u}$, where $x_{1,u}$ is the position of the D_0 channel (i.e., the value of x_1) in the case where the elemental volumes are distributed uniformly. In the present case, where there are only two elemental volumes, uniform distribution means to place the D_0-thin channels exactly halfway between the vertical sides of the system. In the optimization of Fig. 1 and more complex configurations, we used the relative nonuniform/uniform ratios for the positions of channels that can be moved freely,

$$\hat{x}_i = x_i/x_{i,u}. \tag{7}$$

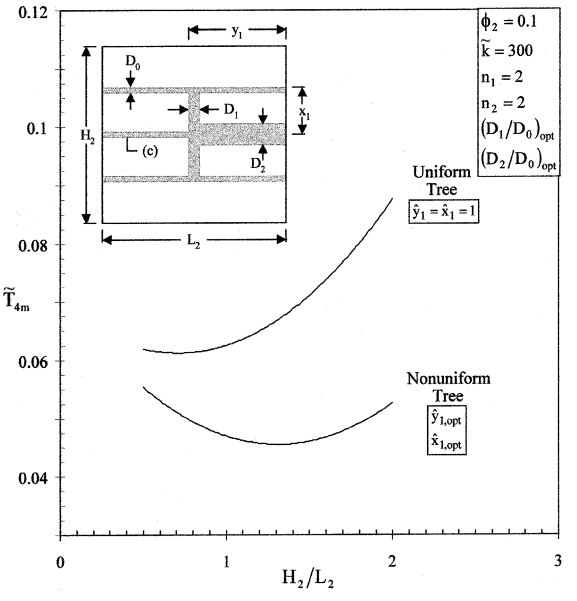

Fig. 4. The optimization of the external shape of a second construct, showing the lowering of the global resistance when the optimized tree channels are distributed nonuniformly ($n_1 = 2$, $n_2 = 2$, $\phi_2 = 0.1$, $\tilde{k} = 300$).

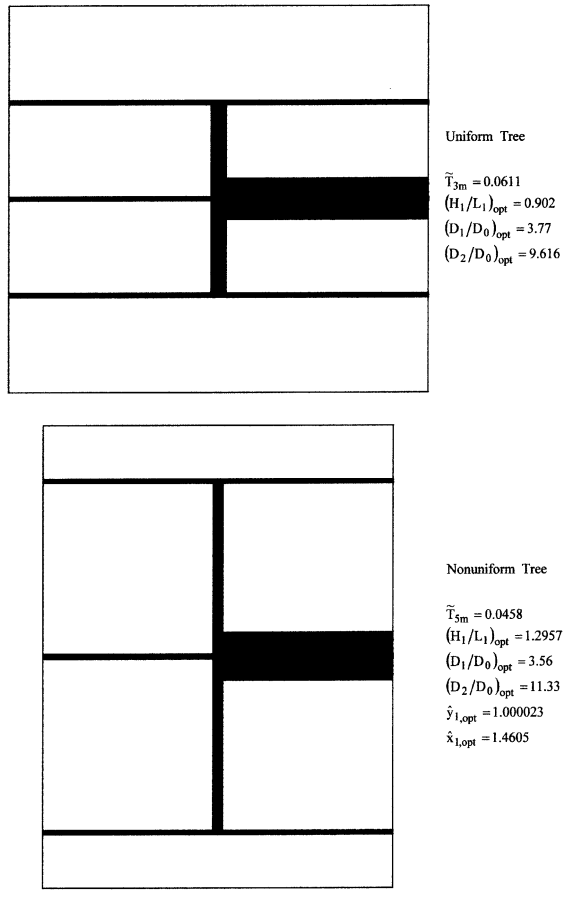

Fig. 5. Optimized second constructs with four elemental volumes, showing the differences between the uniformly and nonuniformly distributed designs ($n_1 = 2$, $n_2 = 2$, $\phi_2 = 0.1$, $\tilde{k} = 300$).

Fig. 2 shows the last phase of the optimization of the first construct with two elements. The global thermal resistance plotted on the ordinate has been minimized already with respect to H_1/L_1 and D_1/D_0 ($\tilde{T}_{2m}$ means that $\tilde{T}_{peak}$ has been minimized twice). The third degree of freedom ($\hat{x}_1$) is optimized in the figure. The optimal location ($\hat{x}_{1,opt} = 1.059$) shows that the best configuration is one with nonuniform distribution of interstitial space. The k_0 interstices that are closer to the root of the k_p tree are thicker. This effect is illustrated on the left side of Fig. 3, which shows a scale drawing of the $n_1 = 2$ first construct in the uniform design (top) and the nonuniform design (bottom). Each frame represents only one half of the construct. The global resistance of the nonuniform structure is 0.7% smaller than the resistance of the uniform structure.

The remainder of Fig. 3 documents the corresponding changes in configuration when the uniform distribution of elements is replaced by an optimized nonuniform distribution in first constructs with $n_1 = 4$ and $n_1 = 6$ elements. Comparing each pair of frames aligned vertically, we see that in the lower frames the elemental channels have migrated away from the plane of the root of the k_p tree. The global performance improvement due to the increased design freedom (the nonuniform distribution) is a 3.6% drop in global ther-

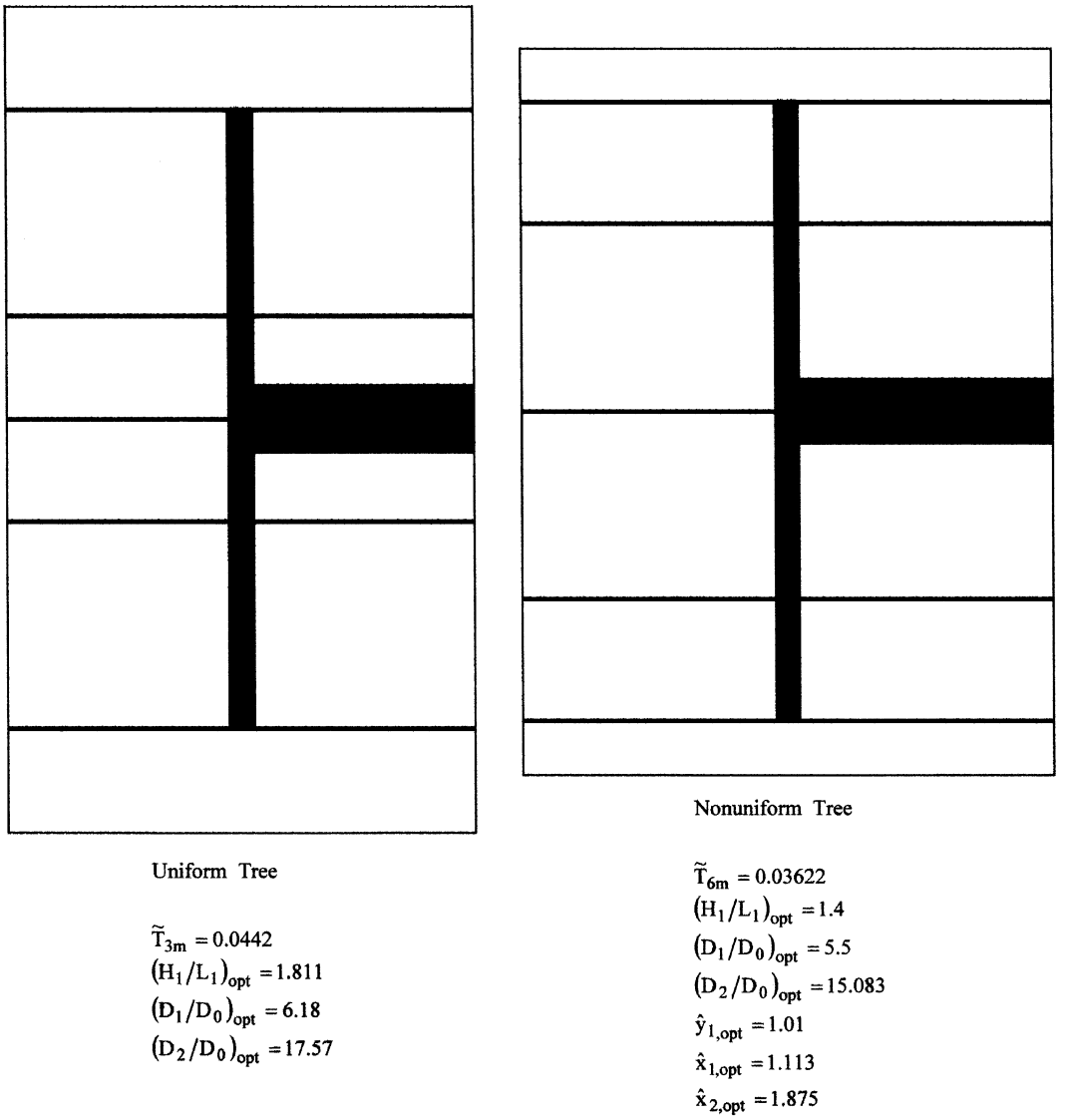

Fig. 6. Optimized second construct with eight elemental volumes, showing the differences between the uniformly and nonuniformly distributed designs ($n_1 = 4$, $n_2 = 2$, $\phi_2 = 0.1$, $\tilde{k} = 300$).

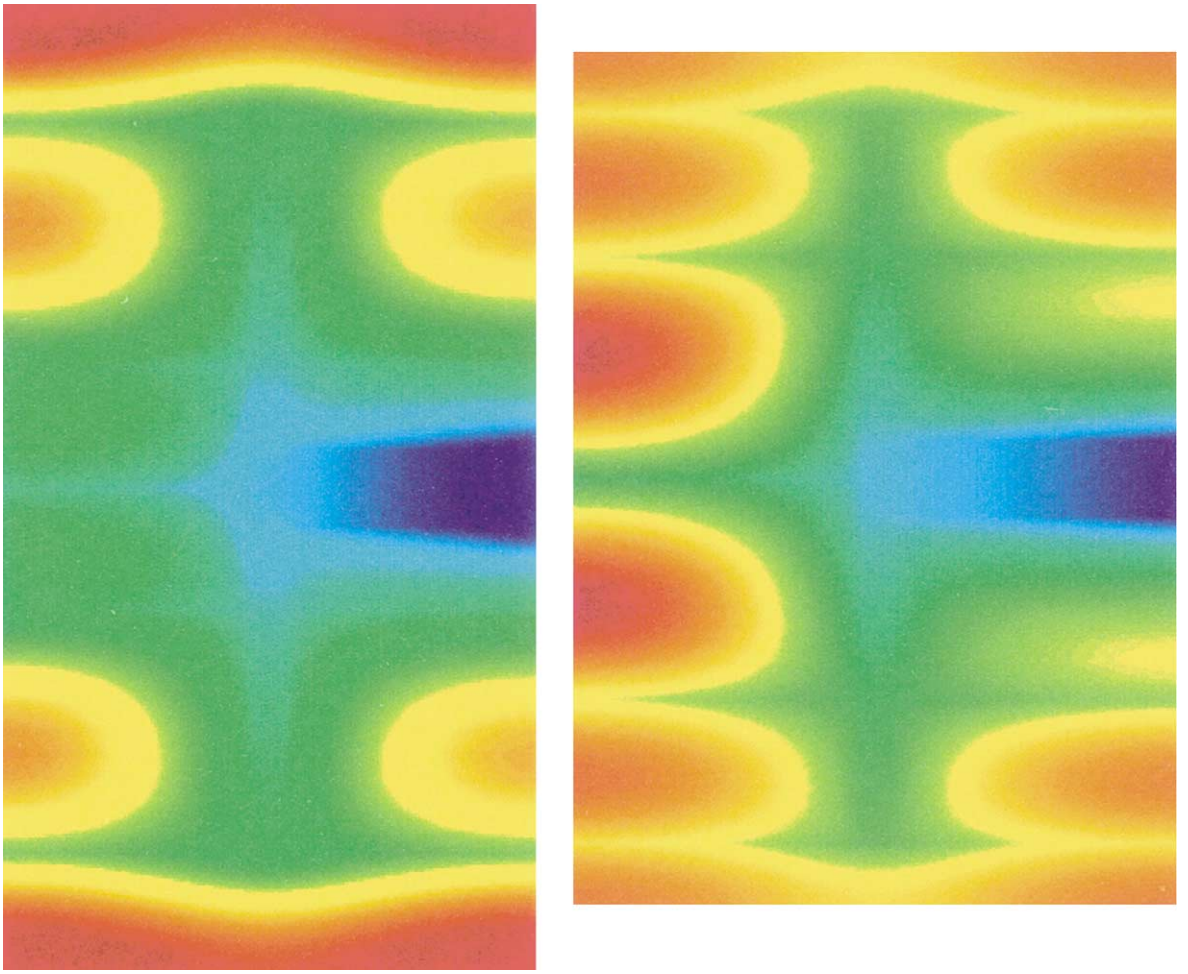

Fig. 6 (*continued*)

mal resistance when $n_1 = 4$, and a 5.7% drop when $n_1 = 6$. Proceeding from left to right in Fig. 3, we see that the relative improvement in performance increases as the complexity (n_1) of the nonuniform construct increases.

4. Second construct with nonuniform interstices

A second construct is an assembly of first constructs, such that a new channel (e.g., D_2 in Fig. 4) collects the heat currents collected by D_1-thin channels. The simplest second construct has only two ($n_2 = 2$) first constructs, and, as we saw in the preceding section, the simplest first construct has only two ($n_1 = 2$) elemental volumes. Putting these two steps of dichotomy (pairing, bifurcation) together, we arrive at the simplest second construct, which is shown in the detail of Fig. 4. There are five, not four ($n_1 n_2 = 4$) elemental volumes in this configuration, as a fifth elemental channel [(c) in Fig. 4] has been added to prevent the formation of a hot spot in the region that is now covered by the tip of the (c) channel. All the designs optimized in this section refer to a composite material with $\tilde{k} = k_p/k_0 = 300$ and $\phi_2 = A_{p2}/A_2 = 0.1$, which means that the high-conductivity material occupies 10% of the entire system volume.

The optimization of the geometry of Fig. 4 has five degrees of freedom, which are represented by D_1/D_0, D_2/D_0, $\hat{y}_1$, $\hat{x}_1$ and H_2/L_2. Note that the ratio $\hat{y}_1 = y_1/y_{1u}$ accounts for the position of the D_1-thin channels relative to the root. The search for the optimal configuration was conducted in a sequence of five optimization loops. The global resistance minimized with respect to the first four degrees of freedom ($\tilde{T}_{4m}$) can be minimized with respect to the fifth (H_2/L_2) as shown by the 'nonuniform tree' curve in Fig. 4. The resulting configuration has been drawn to scale in the lower part of Fig. 5. The upper part of Fig. 5 shows the corresponding structure of the

uniform design ($\hat{x}_1 = \hat{y}_1 = 1$). The global resistance of the optimized nonuniform tree is 25% smaller than the resistance of the optimized uniform tree. This improvement, which is significant, is also visible in Fig. 4, where the upper curve shows the optimization of the uniform design with respect to the external aspect ratio H_2/L_2.

Comparing the two frames of Fig. 5 we conclude that the optimization of global performance forces the tree to become nonuniform, such that the interstices that are closer to the periphery of the corona (away from the root) are smaller. The length of the trunk, however, is the same in the nonuniform design and the corresponding uniform design (note $\hat{y}_{1,\mathrm{opt}} \cong 1$).

Better performance is also achieved through the increase of internal complexity [13]. In Fig. 6 we see the optimized uniform and nonuniform designs of a second construct with a total of eight elemental volumes, i.e., twice as many elemental volumes as in Fig. 5. The global resistances minimized in Fig. 6 are 25% lower than the corresponding thermal resistances of the designs

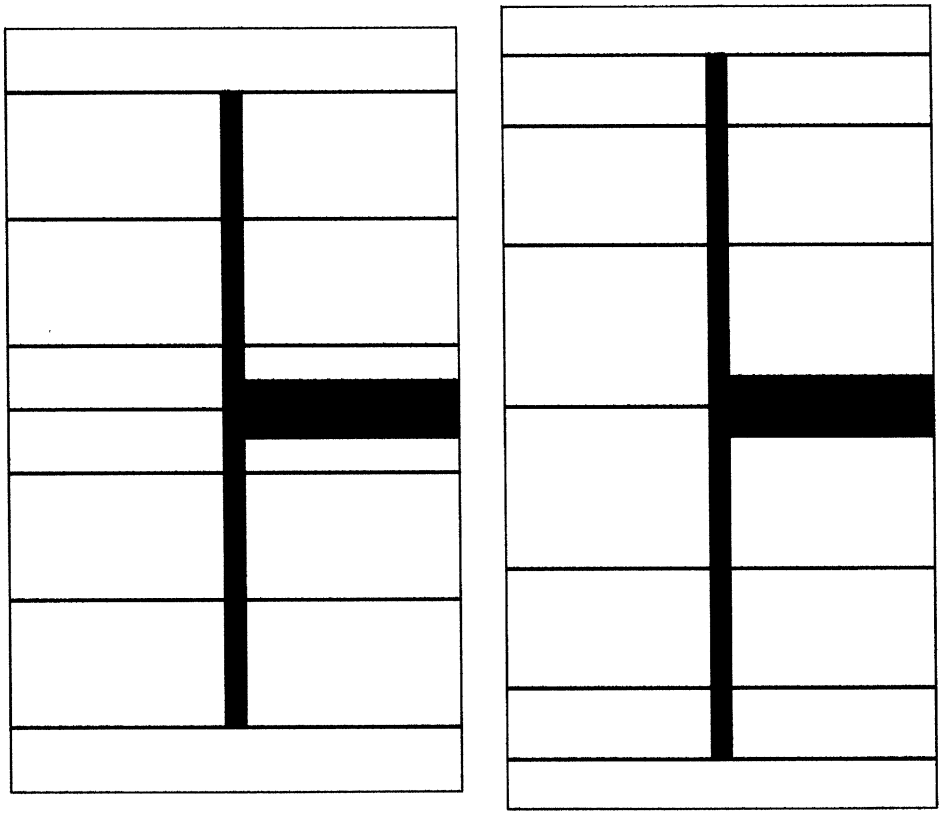

Uniform Tree

$\tilde{T}_{3m} = 0.03776$
$(H_1/L_1)_{opt} = 1.734$
$(D_1/D_0)_{opt} = 7.383$
$(D_2/D_0)_{opt} = 21.018$

Nonuniform Tree

$\tilde{T}_{7m} = 0.03325$
$(H_1/L_1)_{opt} = 1.914$
$(D_1/D_0)_{opt} = 7.523$
$(D_2/D_0)_{opt} = 22.929$
$\hat{y}_{1,opt} = 1.000025$
$\hat{x}_{1,opt} = 1.057$
$\hat{x}_{2,opt} = 1.399$
$\hat{x}_{3,opt} = 2.395$

Fig. 7. Optimized second construct with 12 elemental volumes, showing the differences between the uniformly and nonuniformly distributed designs ($n_1 = 6$, $n_2 = 2$, $\phi_2 = 0.1$, $\tilde{k} = 300$).

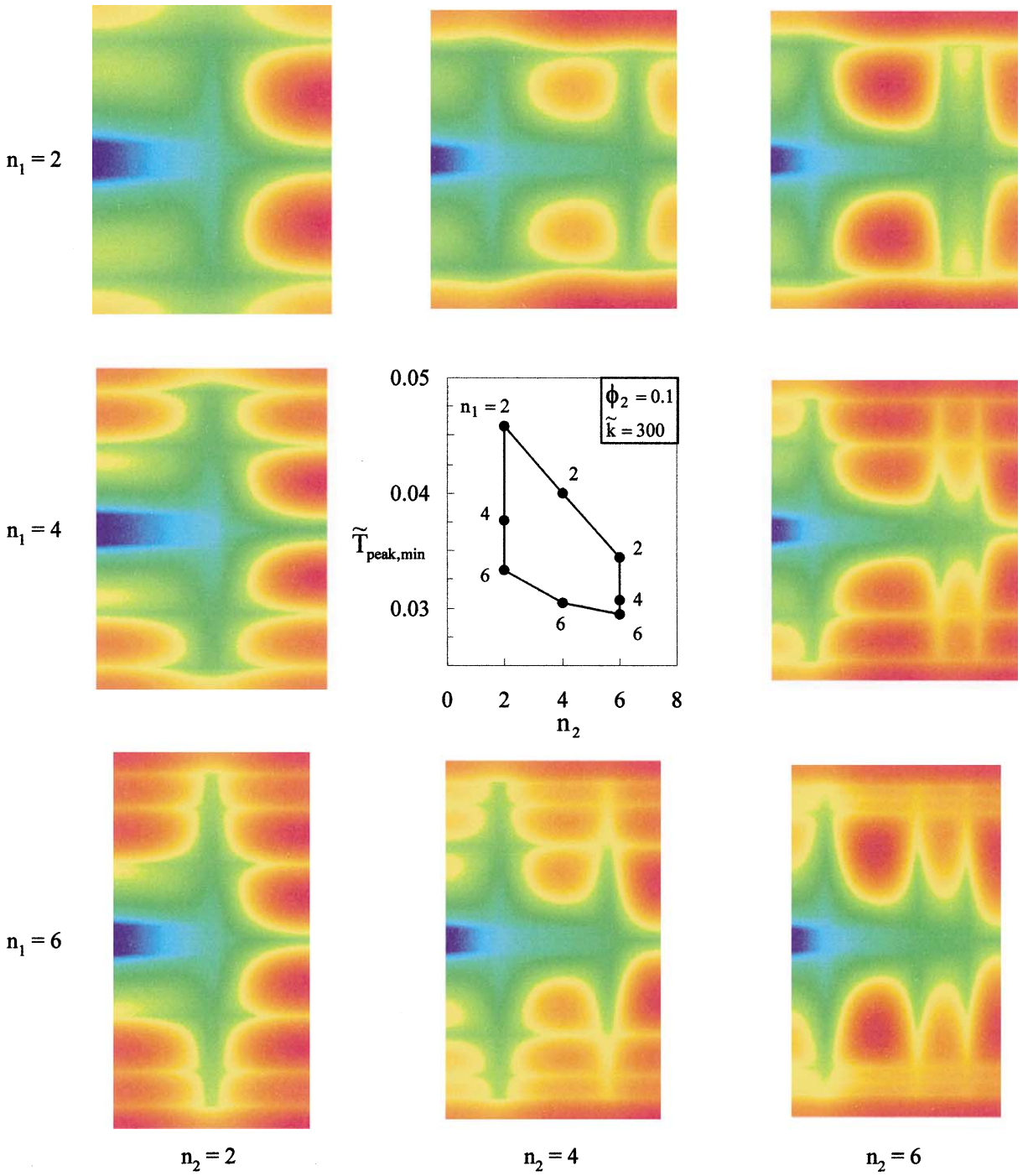

Fig. 8. Optimized second constructs with nonuniform distribution of interstitial sizes, showing two routes to better global performance via optimization of geometric form ($\phi_2 = 0.1$, $\tilde{k} = 300$).

optimized in Fig. 5. These are significant improvements in global performance: if the pursuit of better global performance subject to constraints is a universal principle in nature and engineering, then, *in time*, geometric changes will continue to occur, and complexity will continue to increase [1].

5. Discussion

Optimal distribution of imperfection is another way to describe the constructal principle that generates the optimal structure. The color version of Fig. 6 shows that the effect of switching from the uniformly distributed design to the less constrained, nonuniform design is to spread the imperfection [the high resistance, between the hot spot (red) and the root] more uniformly. It is important to keep in mind that, in every design, even in the uniform tree on the left side of the figure, the hot spots have been spread around as much as possible (note the nearly uniform red color along the top and bottom sides of the left side of Fig. 6). This was achieved through the optimization of the external shape (H_2/L_2) and internal aspect ratios (D_1/D_0, D_2/D_0) of the system with elemental volumes of one size.

The right side of the color figure shows that when more freedom is added to the design the global resistance drops significantly (by 18%), and the hot spots occur almost everywhere in the peripheral regions of the system. We may also say that the nonuniform tree structure even looks 'better' and 'more natural', because its peripheral elements are smaller than the elements found in the vicinity of the trunk. These characteristics are accentuated further in Fig. 7, which shows the corresponding comparison between the optimized uniform and nonuniform designs when the total number of elemental volumes is 12.

Fig. 8 provides a bird's-eye view of how the increase in complexity leads to better global performance and structures with smaller volume elements in the regions far from the root of the high-conductivity tree. Each second construct shown in Fig. 8 was optimized with respect to all its degrees of freedom. The total number of degrees of freedom increased from five in the design in the upper-left corner, to nine in the design in the lower-right corner. Complexity can be increased along two routes, by increasing the number of elements (n_1) in each first construct and keeping the number of first constructs (n_2) fixed, or by increasing the number of first constructs and keeping the number of elements constant at the first-construct level. Either way, the improvement in global performance is significant.

The most complex, nonuniform tree structure is the one in the lower-right corner of Fig. 8. The blue-green vertical branches indicate the axes of the six first constructs. They show that in the nonuniform design the nonuniform distribution of volume elements brings with it a nonuniform distribution of first constructs. The structure is finer in every detail (elements, first constructs) in regions situated farther from the root of the tree. The optimized structure does such a good job of spreading the imperfection around that the color red fills more than half of the volume, and the elemental volumes are almost indistinguishable.

Acknowledgements

This work was supported by a grant from the National Science Foundation and the Ministry of Higher Education, Riyadh, Saudi Arabia.

References

[1] A. Bejan, Shape and Structure, from Engineering to Nature, Cambridge University Press, Cambridge, UK, 2000.
[2] N. MacDonald, Trees and Networks in Biological Models, Wiley, Chichester, UK, 1983.
[3] E.R. Weibel, Morphometry of the Human Lung, Academic Press, New York, 1963.
[4] D'A.W. Thompson, On Growth and Form, Cambridge University Press, Cambridge, UK, 1942.
[5] D.L. Cohn, Optimal systems: I. The vascular system, Bulletin of Mathematical Biophysics 16 (1954) 59–74.
[6] A.E. Scheidegger, Theoretical Geomorphology, second ed., Springer, Berlin, 1970.
[7] L.B. Leopold, M.G. Wolman, J.P. Miller, Fluvial Processes in Geomorphology, Freeman, San Francisco, 1964.
[8] A.L. Bloom, Geomorphology, Prentice-Hall, Englewood Cliffs, NJ, 1978.
[9] T.A. Wilson, Design of the bronchial tree, Nature 213 (1967) 668–669.
[10] R.J. Chorley, S.A. Schumm, D.E. Sugden, Geomorphology, Methuen, London, 1984.
[11] A. Bejan, Constructal-theory network of conducting paths for cooling a heat generating volume, International Journal of Heat and Mass Transfer 40 (1997) 799–816.
[12] FIDAP 8.01, Theory Manual, Fluent Inc., 1998.
[13] A. Bejan, N. Dan, Two constructal routes to minimal heat flow resistance via greater internal complexity, Journal of Heat Transfer 121 (1999) 6–14.